

Spin torque oscillator based on magnetic tunnel junction with MgO cap layer for radio-frequency-oriented neuromorphic computing

Huayao Tu(涂华垚), Yanxiang Luo(雒雁翔), Kexin Zeng(曾柯心), Yuxuan Wu(吴宇轩), Like Zhang(张黎可), Baoshun Zhang(张宝顺), and Zhongming Zeng(曾中明)
Citation: Chin. Phys. B, 2023, 32 (**10**): 107504. DOI: 10.1088/1674-1056/acb424
Journal homepage: http://cpb.iphy.ac.cn; http://iopscience.iop.org/cpb

What follows is a list of articles you may be interested in

From microelectronics to spintronics and magnonics

Xiu-Feng Han(韩秀峰), Cai-Hua Wan(万蔡华), Hao Wu(吴昊), Chen-Yang Guo(郭晨阳), Ping Tang(唐萍), Zheng-Ren Yan(严政人), Yao-Wen Xing(邢耀文), Wen-Qing He(何文卿), and Guo-Qiang Yu(于国强)
Chin. Phys. B, 2022, 31 (**11**): 117504. DOI: 10.1088/1674-1056/ac9048

Experiments and SPICE simulations of double MgO-based perpendicular magnetic tunnel junction

Qiuyang Li(李求洋), Penghe Zhang(张蓬鹤), Haotian Li(李浩天), Lina Chen(陈丽娜), Kaiyuan Zhou(周恺元), Chunjie Yan(晏春杰), Liyuan Li(李丽媛), Yongbing Xu(徐永兵), Weixin Zhang(张卫欣), Bo Liu(刘波), Hao Meng(孟浩), Ronghua Liu(刘荣华), and Youwei Du(都有为)
Chin. Phys. B, 2021, 30 (**4**): 047504. DOI: 10.1088/1674-1056/abdea2

Strong anti-strain capacity of CoFeB/MgO interface on electronic structure and state coupling

Fei Guo(郭飞), Yaping Wu(吴雅苹), Zhiming Wu(吴志明), Ting Chen(陈婷), Heng Li(李恒), Chunmiao Zhang(张纯淼), Mingming Fu(付明明), Yihong Lu(卢奕宏), Junyong Kang(康俊勇)
Chin. Phys. B, 2018, 27 (**1**): 017502. DOI: 10.1088/1674-1056/27/1/017502

Perpendicular magnetic tunnel junction and its application in magnetic random access memory

Liu Hou-Fang (刘厚方), Syed Shahbaz Ali, Han Xiu-Feng (韩秀峰)
Chin. Phys. B, 2014, 23 (**7**): 077501. DOI: 10.1088/1674-1056/23/7/077501

Spin torque oscillator based on magnetic tunnel junction with MgO cap layer for radio-frequency-oriented neuromorphic computing

Huayao Tu(涂华垚)[1,2], Yanxiang Luo(雒雁翔)[1,2], Kexin Zeng(曾柯心)[1,2,5], Yuxuan Wu(吴宇轩)[1,2], Like Zhang(张黎可)[3,†], Baoshun Zhang(张宝顺)[2], and Zhongming Zeng(曾中明)[1,2,4,‡]

[1] *School of Nano Technology and Nano Bionics, University of Science and Technology of China, Hefei* 230026, *China*
[2] *Nanofabrication Facility, Suzhou Institute of Nano-Tech and Nano-Bionics, Chinese Academy of Sciences, Suzhou* 215123, *China*
[3] *School of Electronics and Information Engineering, Wuxi University, Wuxi* 214105, *China*
[4] *Nanchang (SINANONC) Nano-Devices and Technologies Division, Suzhou Institute of Nano-Tech and Nano-Bionics, Chinese Academy of Sciences, Nanchang* 330200, *China*
[5] *Nano Science and Technology Institute, University of Science and Technology of China, Suzhou* 215123, *China*

(Received 1 November 2022; revised manuscript received 12 January 2023; accepted manuscript online 18 January 2023)

Recently, it has been proposed that spin torque oscillators (STOs) and spin torque diodes could be used as artificial neurons and synapses to directly process microwave signals, which could lower latency and power consumption greatly. However, one critical challenge is to make the microwave emission frequency of the STO stay constant with a varying input current. In this work, we study the microwave emission characteristics of STOs based on magnetic tunnel junction with MgO cap layer. By applying a small magnetic field, we realize the invariability of the microwave emission frequency of the STO, making it qualified to act as artificial neuron. Furthermore, we have simulated an artificial neural network using STO neuron to recognize the handwritten digits in the Mixed National Institute of Standards and Technology database, and obtained a high accuracy of 92.28%. Our work paves the way for the development of radio-frequency-oriented neuromorphic computing systems.

Keywords: spin torque oscillators, artificial neuron, neuromorphic computing, magnetic tunnel junctions

PACS: 75.76.+j, 72.25.–b, 85.75.–d **DOI:** 10.1088/1674-1056/acb424

1. Introduction

By emulating a biological brain, neuromorphic computing is considered to be the future of artificial intelligence (AI).[1,2] In comparison with the traditional von Neumann architecture, where the computing and memory components are separated, neuromorphic computing implements a centralized strategy. The data are processed directly in or close to memory, which will greatly reduce the power consumption resulting from data movement, particularly when performing complex cognitive tasks. Although the algorithms of artificial neural networks (ANNs) have made great progress in solving many problems,[3] the lack of dedicated hardware has hindered the further development of neuromorphic computing. Thus, much effort has been committed to exploring novel materials and structures for potential application in neuromorphic computing. So far, many materials solutions have been put forward, including phase change materials,[4] ferroelectric materials,[5,6] spintronic materials,[7,8] resistive memory,[9,10] and two-dimensional materials.[11,12] Among these, spintronic devices stand out due to their high speed, high endurance, nanoscale size, lower power consumption and excellent CMOS compatibility.[13,14] In particular, magnetic tunnel junctions (MTJs), the most representative spintronic device, have recently been demonstrated to possess huge potential in neuromorphic computing. Many inspiring works have been reported, including multilevel synapses based on spin torque memristors, neuromorphic computing based on the synchronization of spin oscillators, artificial neurons of ANNs based on spin torque stochastic switching and microwave detection, and spiking neurons with superparamagnetic tunnel junctions, etc.[15–19]

More recently, it has been proposed numerically and proved experimentally that MTJ-based spin torque diodes (STDs) can act as spintronic synapses and carry out radio-frequency (RF) multiply-and-accumulate (MAC) operation by rectifying the input microwave power into direct voltages.[20,21] Correspondingly, spin torque oscillators (STOs) can be used as artificial neurons and perform nonlinear activation through converting the direct current into microwave power.[22,23] Considering the wide application of RF signals in information communication and the increasing demand for wireless communication, it would be really appealing to develop such compact and energy efficient RF hardware system for intelligent RF signals processing. However, there exists one critical problem with STOs. It is required that the microwave emission frequency does not change with varying

†Corresponding author. E-mail: lkzhang@cwxu.edu.cn
‡Corresponding author. E-mail: zmzeng2012@sinano.ac.cn

© 2023 Chinese Physical Society and IOP Publishing Ltd

current, while STOs typically have a dependence on input direct current.

Here, we study the microwave emission properties of STOs based on MTJs with MgO cap layer. By applying a specific magnetic field, the emission frequency of the STO can stay unchanged with the increase of drive d.c. current, which meets the requirement of an RF-oriented artificial neuron. Furthermore, a neural network constructed with the STO neuron is used to solve the Mixed National Institute of Standards and Technology (MNIST) handwritten digits recognition problem. A high accuracy of up to 92.28% is achieved.

2. Materials and methods

As depicted in Fig. 1, the MTJ stacks used in this work consist of a bottom electrode, a core structure of PtMn (15)/$Co_{70}Fe_{30}$ (2.3)/Ru (0.85)/$Co_{40}Fe_{40}B_{20}$ (2.4)/MgO (1)/$Co_{20}Fe_{60}B_{20}$ (2.0)/MgO (0.7) and a top electrode (thicknesses in nm). The MgO cap layer here is used to induce additional interfacial perpendicular magnetic anisotropy, lowering the demagnetization field and damping factor.[24,25] The thin films were deposited on a thermally oxidized silicon substrate using a magnetron sputtering system and annealed at 300 °C for 2.0 h in an in-plane magnetic field of 1 T. The magnetization direction of the pinned synthetic antiferromagnet (SAF) of $Co_{70}Fe_{30}$/Ru/$Co_{40}Fe_{40}B_{20}$ is magnetically hardened so that it can serve as the reference layer (RL) while the direction of magnetization of the Fe-rich $Co_{20}Fe_{60}B_{20}$ layer, called the free layer (FL), is free to rotate. Using electron beam lithography and Ar ion beam milling, the MTJ was defined and etched into a 150 nm×70 nm elliptical nano-pillar with its long axis parallel to the magnetic field for annealing. The microwave emission is measured on a spectrum analyzer after 40 dB amplification. The background noise, quantified at zero bias current, has been subtracted from the microwave emissions. All the data were measured at room temperature.

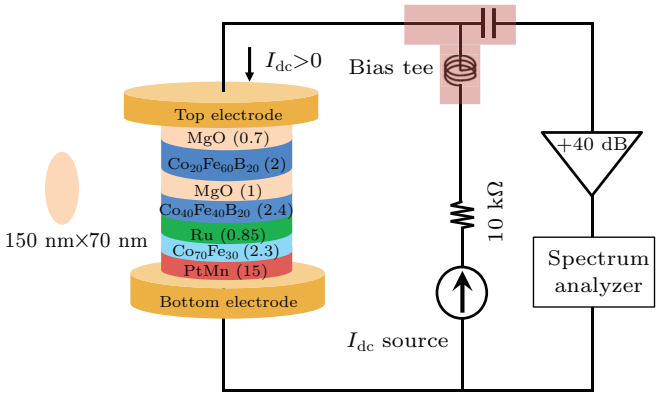


Fig. 1. The core structure of the device (numbers in the parentheses indicate the thickness in nm) and the experimental measurement setup used in this work.

3. Results and discussion

First, we characterize the static transport properties of the device. Figure 2 shows the magnetoresistance as a function of the in-plane magnetic field applied along the magnetic easy axis and hard axis at a bias current of 10 μA. It can be seen that, as the field H_{easy} increases from negative to positive values, the resistance abruptly changes from a low-resistance state ($R_P = 547\ \Omega$) to a high-resistance one ($R_{AP} = 1095\ \Omega$). This indicates that the relative magnetization configuration between the free layer and pinned layer changes from a parallel (P) to an antiparallel (AP) state. Correspondingly, the magnetoresistance ratio, defined as $(R_{AP} - R_P)/R_P$, is calculated to be 100%, suggesting the good quality of our device. As for the resistance in the hard axis, the resistance gradually saturates with increasing field, indicating that the magnetization rotates towards the hard axis at larger fields.

Next, we investigate the microwave emission characteristic of the device with magnetic field applied along the in-plane hard axis. Figure 2(b) presents the microwave emission spectra under different driven currents at three magnetic fields. As the field increases from −200 Oe to −400 Oe, the relationship between microwave frequency and current changes from an apparently negative one to a slightly positive one, with the frequency remaining constant at −300 Oe. According to the nonlinear auto-oscillator theory,[22,26–28] the dependence of frequency on drive current can be described as follows:

$$f(I_{dc}) = f_{FMR} + \frac{N}{2\pi}P, \tag{1}$$

where N is the nonlinearity factor and P is the normalized power of the stationary precession. In our case, it is obvious that we have successfully tuned the nonlinearity from a negative value to a positive one by changing the magnitude of the magnetic field. Such field dependence is consistent with the results reported before.[29–32] In addition, it has been reported that the nonlinearity can be reduced by compensating the demagnetization field.[33] In our device, the additional CoFeB–MgO cap interface will induce IPMA, which acts against the demagnetization field.[24,25] Hence, the reduction of demagnetization field due to the MgO cap layer may also contribute to the invariance of frequency. The reason why the dashed line moves first to a low frequency and then moves back to high frequency with increasing magnetic field may be due to the influence of the synthetic antiferromagnet layers.[34]

To give a clearer view of the current dependence of microwave frequency, we have plotted some typical power density spectra under different currents in Fig. 3(a). By extracting the experimental data, the frequency and total integrated power of the oscillation as a function of $|I_{dc}|$ are shown in Fig. 3(b). It is apparent that the emission frequency remains constant at around 1.95 GHz with some slight deviation of less than 0.02 GHz at low currents. The emission power exhibits ReLU-like nonlinear output characteristics. Therefore, our device meets the requirement for carrying out AI computation directly with a microwave signal.

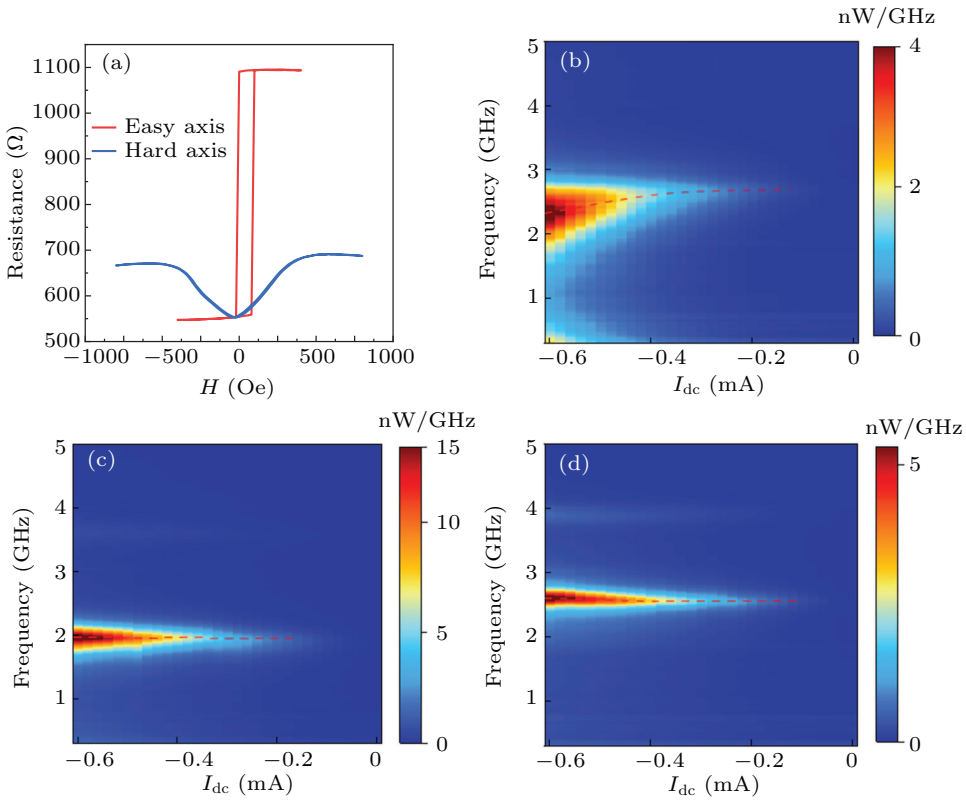


Fig. 2. (a) Magnetoresistances of the device versus magnetic field at a bias current of 10 μA. (b) Microwave emission spectra under different driven currents with a magnetic field of (b) −200 Oe, (c) −300 Oe and (d) −400 Oe, respectively, where the dashed lines show the central emission frequency of the device.

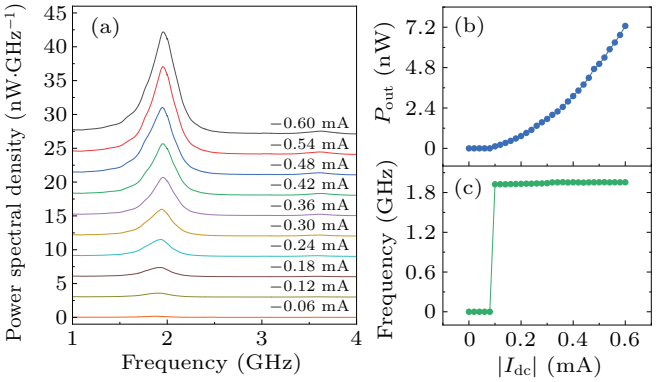


Fig. 3. (a) The power density spectra measured at different bias currents under a magnetic field of −300 Oe. The microwave (c) emission frequencies and (b) total integrated output power of the STO as a function of the driven currents at −300 Oe.

To demonstrate the potential of the STO artificial neuron, a three-layer ANN is constructed using PyTorch software to recognize the widely used MNIST database of handwritten digits.[35] The database includes 60000 and 10000 images for training and testing processes, respectively. Figure 4(a) depicts the structure of the neural network, consisting of one input layer, one hidden layer and one output layer with 784, 100 and 10 neurons, respectively. Each image in the database has 28×28 pixels, corresponding to 784 input neurons, while the 10 output neurons correspond to the ten digits from 0 to 9. All the neurons are assumed to share the same characteristics obtained from the experimental data, as shown in Fig. 3(b), to speed up the training process. Before being fed into the neural network, the images are randomly divided into multiple batches with each batch containing 256 images. The back-propagation algorithm and stochastic gradient descent are used to minimize the cross-entropy loss with the learning rate being 0.01. It is noted that the experimental data cannot emulate any known software activation function. So, the gradient is calculated numerically using the method described in Ref. [36]. It should be stressed that neuron-to-neuron variability exists in the real hardware implementation of STO-based artificial neurons and further study on its impact is needed in the future. By training the network 50 times and calculating the average, we obtain the dependence of the recognition rate on training epochs, as shown in Fig. 4. The recognition accuracy of the STO-based ANN is up to 92.28%, which is comparable to the accuracy of 94.72% acquired from an ANN having the same structure but with ReLU as the activation function. The results suggest the great potential of the proposed STO-based ANN for RF-oriented neuromorphic computing.

The above results confirm that invariability of the microwave emission frequency can be realized by applying a small magnetic field in the MTJ with a MgO cap layer. It is also worth noting that the required magnetic field can be provided by a magnetic hard mask.[37] such as Co, which makes it more practical for the real-world implementation of the device. We emphasize that our study offers a universal path to solve one of the key issues in utilizing STOs as artificial neurons to directly process RF signals. As for the varied frequencies in STO arrays, some methods should be adopted to intentionally tune the emission frequency. For example, one can change the

free layer by adding a memristive layer or ferroelectric layer to the structure.[38,39]

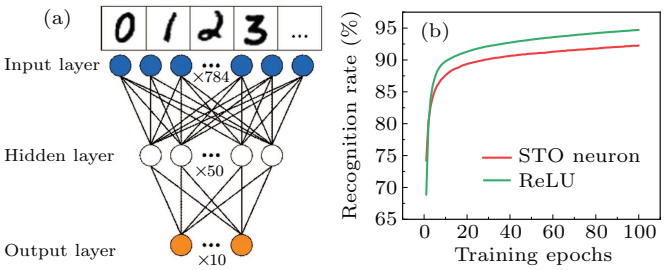


Fig. 4. (a) The structure of the ANN consisting of three layers, with 784, 100 and 10 neurons for the input layer, hidden layer and output layer, respectively. (b) The recognition accuracy of the inference dataset versus training epochs obtained from the ANN constructed with a STO, compared with a conventional ANN with the ReLU activation function. Both results are averages from 50 runs.

4. Conclusion

In this work, we have investigated the microwave emission properties of a STO based on an MTJ with a MgO cap layer. We found that when a weak magnetic field is applied the device can maintain an invariable emission frequency, making it suitable for RF-oriented neuromorphic computing. Using STO as artificial neuron, we have simulated a three-layer ANN to recognize the handwritten digits in the MINST database. A high accuracy of 92.28% is achieved, comparable to the 94.72% obtained with a conventional ANN constructed with ReLU software neurons. Our work may provide inspiration for the development of RF-oriented neuromorphic computing.

Acknowledgements

The authors are grateful for the technical support for Nano-X from Suzhou Institute of Nano-Tech and Nano-Bionics, Chinese Academy of Sciences (SINANO).

Project supported by the National Natural Science Foundation of China (Grant Nos. 11974379 and 12204357), K. C. Wong Education Foundation (Grant No. GJTD-2019-14), Jiangxi Province "Double Thousand Plan" (Grant No. S2019CQKJ2638), the Natural Science Foundation of the Jiangsu Higher Education Institutions of China (Grant No. 22KB140017), and Wuxi University Research Start-up Fund for Introduced Talents (Grant No. 2022r006).

References

[1] Marković D, Mizrahi A, Querlioz D and Grollier J 2020 *Nat. Rev. Phys.* **2** 499
[2] Roy K, Jaiswal A and Panda P 2019 *Nature* **575** 607
[3] LeCun Y, Bengio Y and Hinton G 2015 *Nature* **521** 436
[4] Boybat I, Le Gallo M, Nandakumar S R, Moraitis T, Parnell T, Tuma T, Rajendran B, Leblebici Y, Sebastian A and Eleftheriou E 2018 *Nat. Commun.* **9** 2514
[5] Luo Z D, Yang M M, Liu Y and Alexe M 2021 *Adv. Mater.* **33** 2005620
[6] Jaiswal A, Agrawal A, Panda P and Roy K 2021 *IEEE T. Magn.* **57** 4300209
[7] Grollier J, Querlioz D, Camsari K Y, Everschor-Sitte K, Fukami S and Stiles M D 2020 *Nat. Electron.* **3** 360
[8] Romera M, Talatchian P, Tsunegi S, Abreu Araujo F, Cros V, Bortolotti P, Trastoy J, Yakushiji K, Fukushima A, Kubota H, Yuasa S, Ernoult M, Vodenicarevic D, Hirtzlin T, Locatelli N, Querlioz D and Grollier J 2018 *Nature* **563** 230
[9] Xue C X, Chiu Y C, Liu T W, Huang T Y, Liu J S, Chang T W, Kao H Y, Wang J H, Wei S Y, Lee C Y, Huang S P, Hung J M, Teng S H, Wei W C, Chen Y R, Hsu T H, Chen Y K, Lo Y C, Wen T H, Lo C C, Liu R S, Hsieh C C, Tang K T, Ho M S, Su C Y, Chou C C, Chih Y D and Chang M F 2021 *Nat. Electron.* **4** 81
[10] Ielmini D and Wong H S P 2018 *Nat. Electron.* **1** 333
[11] Cao G M, Meng P, Chen J G, Liu H S, Bian R J, Zhu C, Liu F C and Liu Z 2020 *Advanced Functional Materials* **31** 2005443
[12] Huh W, Lee D and Lee C H 2020 *Adv. Mater.* **32** 2002092
[13] Cai W, Shi K, Zhuo Y, Zhu D, Huang Y, Yin J, Cao K, Wang Z, Guo Z, Wang Z, Wang G and Zhao W 2021 *IEEE Electron Device Letters* **42** 704
[14] Fong X Y, Kim Y S, Yogendra K, Fan D L, Sengupta A, Raghunathan A and Roy K 2016 *IEEE Transactions on Computer-Aided Design of Integrated Circuits and Systems* **35** 1
[15] Cai J L, Fang B, Wang C and Zeng Z M 2017 *Appl. Phys. Lett.* **111** 182410
[16] Lv H, Fidalgo J, Silva A V, Leitao D C, Kampfe T, Langer J, Wrona J, Ocker B, Freitas P P and Cardoso S 2020 *Adv. Electron. Mater.* **7** 2000976
[17] Zhang X, Cai W, Wang M, Pan B, Cao K, Guo M, Zhang T, Cheng H, Li S, Zhu D, Wang L, Shi F, Du J and Zhao W 2021 *Adv. Sci.* **8** 2004645
[18] Shi K, Cai W, Jiang S, Zhu D, Cao K, Guo Z, Wei J, Du A, Li Z, Huang Y, Yin J, Åkerman J and Zhao W 2021 *Science China Physics, Mechanics & Astronomy* **65** 227511
[19] Cai W, Wang M, Cao K, Yang H, Peng S, Li H and Zhao W 2021 *Science China Information Sciences* **65** 122406
[20] Leroux N, Marković D, Martin E, Petrisor T, Querlioz D, Mizrahi A and Grollier J 2021 *Phys. Rev. Appl.* **15** 034067
[21] Leroux N, Mizrahi A, Markovic D, Sanz-Hernandez D, Trastoy J, Bortolotti P, Martins L, Jenkins A, Ferreira R and Grollier J 2021 *Neuromorph. Comput. Eng.* **1** 011001
[22] Slavin A and Tiberkevich V 2009 *IEEE Transactions on Magnetics* **45** 1875
[23] Leroux N, De Riz A, Sanz-Hernández D, Marković D, Mizrahi A and Grollier J 2022 *Neuromorph. Comput. Eng.* **2** 034002
[24] Zhang L K, Fang B, Cai J L and Zeng Z M 2018 *Appl. Phys. Lett.* **112** 242408
[25] Kubota H, Ishibashi S, Saruya T, Nozaki T, Fukushima A, Yakushiji K, Ando K, Suzuki Y and Yuasa S 2012 *J. Appl. Phys.* **111** 07C723
[26] Slavin A and Tiberkevich V 2008 *IEEE Transactions on Magnetics* **44** 1916
[27] Slavin A and Tiberkevich V 2005 *Appl. Rev. Lett.* **95** 237201
[28] Slavin A N and Kabos P 2005 *IEEE Transactions on Magnetics* **41** 1264
[29] Dumas R K, Iacocca E, Bonetti S, Sani S R, Mohseni S M, Eklund A, Persson J, Heinonen O and Åkerman J 2013 *Appl. Rev. Lett.* **110** 257202
[30] Pufall M R, Rippard W H, Russek S E, Kaka S and Katine J A 2006 *Appl. Rev. Lett.* **97** 087206
[31] Rippard W H, Pufall M R and Russek S E 2006 *Phys. Rev. B* **74** 224409
[32] Gerhart G, Bankowski E, Melkov G A, Tiberkevich V S and Slavin A N 2007 *Phys. Rev. B* **76** 024437
[33] Jiang S, Khymyn R, Chung S, Le T Q, Diez L H, Houshang A, Zahedinejad M, Ravelosona D and Åkerman J 2020 *Appl. Phys. Lett.* **116** 072403
[34] Gonççalves A M, Barsukov I, Chen Y J, Yang L, Katine J A and Krivorotov I N 2013 *Appl. Phys. Lett.* **103** 172406
[35] Lecun C C and Burges C J C http://yann.lecun.com/exdb/mnist/
[36] Cai J L, Zhang L K, Fang B, Lv W X, Zhang B S, Finocchio G, Xiong R, Liang S H and Zeng Z M 2019 *Appl. Phys. Lett.* **114** 192402
[37] Garello K, Yasin F, Hody H, Couet S, Souriau L, Sharifi S H, Swerts J, Carpenter R, Rao S, Kim W, Wu J, Sethu K K V, Pak M, Jossart N, Crotti D, Furnemont A and Kar G S 2019 *Symposium on VLSI Technology* 18852132
[38] Zahedinejad M, Fulara H, Khymyn R, Houshang A, Dvornik M, Fukami S, Kanai S, Ohno H and Akerman J 2021 *Nat. Mater.* **21** 81
[39] Liu M, Howe B M, Grazulis L, Mahalingam K, Nan T, Sun N X and Brown G J 2013 *Adv. Mater.* **25** 4886